

## Tight-binding models for hot dense hydrogen

I. Kwon, J. D. Kress, and L. A. Collins

*Theoretical Division, Los Alamos National Laboratory, Los Alamos, New Mexico 87545*

(Received 19 April 1994)

In order to understand the structure and dynamics of hot dense hydrogen, a tight-binding model for hydrogen is developed by fitting the energies of the hydrogen molecule and various crystal structures of solid hydrogen. Pair correlation functions and self-diffusion coefficients obtained from tight-binding molecular-dynamics simulations on relatively large systems for long time scales compare very well with density-functional molecular-dynamics results at various densities ( $0.1\text{--}3\text{ g cm}^{-3}$ ) and temperatures ( $0.1\text{--}5\text{ eV}$ ).

### I. INTRODUCTION

An understanding of hot dense plasmas is important in many areas of physics. For example, in inertial confinement fusion (ICF),<sup>1</sup> the stability and symmetry of target pellets of deuterium and tritium mixtures at densities of hundreds of  $\text{g cm}^{-3}$  and temperatures of  $10^6$  of degrees K are essential for reaching ignition. In astrophysics, the modeling of both stellar<sup>2</sup> and planetary<sup>3</sup> interiors hinges on the properties of dense hydrogen. In particular, augmenting the traditional one-component plasma<sup>4</sup> (OCP) with quantal effects has important ramifications for the evolution and crystallization of white dwarfs.<sup>5</sup>

Recently, there have been several attempts to describe the structure and dynamics of dense hydrogen with molecular-dynamics simulations. To treat particle interactions quantum mechanically, Hartree-Fock<sup>6</sup> and density-functional<sup>7-9</sup> approximations were employed in the electronic structure calculations. These calculations are very accurate but expensive so that small size samples ( $\leq 64$  atoms) were studied at low temperatures [ $\leq 0.1\text{ eV}$  (Refs. 6, 7, and 9) and  $\leq 1\text{ eV}$  (Ref. 8)]. On the other hand, Zérah *et al.*<sup>10</sup> combined the Thomas-Fermi model into molecular-dynamics simulations and studied hydrogen plasmas at higher temperature ( $\simeq 2.5\text{ eV}$ ) with 54 hydrogen atoms.

However, static quantum chemistry calculations on large collections of atoms<sup>11,12</sup> showed that certain properties of dense plasmas such as the width of the electronic energy levels only began to converge after the inclusion of tens to hundreds of atoms in the sample. In addition, models based on an atom in jellium came to similar conclusions.<sup>13</sup> Therefore, to model hot dense plasmas with a large collection of atoms, we aim to develop tight-binding models for hydrogen.

The tight-binding molecular-dynamics (TBMD) method has been utilized in many studies of the structural and dynamical properties of semiconductors in various phases.<sup>14</sup> In this method, the forces governing atomic motions are calculated quantum mechanically including electronic contributions obtained from parametrized tight-binding Hamiltonians. Therefore, quantum-mechanical many-body interactions, which are

crucial to modeling hot dense plasmas,<sup>15,16</sup> are included automatically in the simulations. Moreover, the TBMD method can be applicable to long time simulations on large systems of the order of hundreds of atoms.<sup>15,16</sup>

In this paper, we present a tight-binding model for hydrogen to study the structure and dynamics of hot dense hydrogen plasmas. The details of the model are described in Sec. II, followed by the results of molecular-dynamics simulations in Sec. III, and the summary in Sec. IV.

### II. TIGHT-BINDING MODELS FOR HYDROGEN

In the tight-binding molecular-dynamics (TBMD) scheme, the Hamiltonian governing the atomic motions is

$$H = \sum_i \frac{P_i^2}{2m} + \sum_n \langle \psi_n | H_{\text{TB}} | \psi_n \rangle + \sum_{i>j} \phi(r_{ij}), \quad (1)$$

where the first term is the kinetic energy of ions, the second term is the electronic energy calculated by summing eigenvalues of occupied states from the tight-binding Hamiltonian  $H_{\text{TB}}$ , and  $\phi(r_{ij})$  in the third term is a pairwise potential representing the ion-ion repulsion and the correction for double counting the electron-electron interaction in the second term.

In an earlier approach, Skinner and Pettifor<sup>17</sup> developed a tight-binding model for hydrogen with one  $s$  orbital per hydrogen atom as the basis, by coupling the Harris-Foulkes scheme with Anderson's chemical pseudopotential theory. Although the binding energies of diatomic molecular and solid hydrogen (simple cubic and face-centered-cubic crystal structures) compared well with first principles results, there are shortcomings in the applications for molecular-dynamics simulations of hot dense hydrogen. To study the structure and dynamics at high density ( $\rho \geq 1\text{ g cm}^{-3}$ ) and high temperature ( $T \geq 1\text{ eV}$ ), excited atomic orbitals are necessary in the basis since the probability of electrons to occupy excited states is not negligible. Furthermore, the inclusion of only nearest-neighbor interactions is not practical in

molecular-dynamics simulations where a phase transition from diatomic molecular to atomic liquid phase could occur.

In this paper, we present a tight-binding model for hydrogen which should be applicable to study hot dense hydrogen with molecular-dynamics simulations. We use an orthogonal atomic orbital basis of the ground ( $s$ ) and excited ( $s'$ ) orbitals for each hydrogen atom. First, to fit hopping matrix elements in the tight-binding Hamiltonian, we have performed configuration interaction (CI) calculations<sup>18</sup> for the ground state of the hydrogen molecule ( $^1\Sigma_g^+$ ), its first excited singlet state ( $E, F^1\Sigma_g^+$ ), and triplet excited state ( $^3\Sigma_u^+$ ). These calculations are nearly indistinguishable with those of Kolos and Wolniewicz,<sup>19</sup> except for finer grids especially at short distances. If we assume no interaction between the  $s$  orbital and  $s'$  orbital [ $h_{ss'}(r) \equiv 0$ ], within the tight-binding (Hartree) approximation, we can express

the binding energies of these molecular states as a function of the hopping matrix elements  $h_{ss}(r)$  and  $h_{s's'}(r)$ , and the pair potential  $\phi(r)$ :

$$E(^1\Sigma_g^+, r) = 2h_{ss}(r) + \phi(r), \quad (2)$$

$$E(E, F^1\Sigma_g^+, r) = h_{ss}(r) + h_{s's'}(r) + E_{ss'} + \phi(r), \quad (3)$$

$$E(^3\Sigma_u^+, r) = \phi(r). \quad (4)$$

Here,  $h_{\alpha\beta}(r)$  represents the hopping integral between  $\alpha$  and  $\beta$  orbitals on two interacting hydrogen atoms separated by distance  $r$ , and  $E_{ss'}$  is defined by the difference between on-site energy terms  $E_s$  and  $E_{s'}$ .

In nonlinear fits to CI results, we used the atomic value 10.205 eV for  $E_{ss'}$ . For the hopping integrals, we used the following functions:

$$h_{ss}(r) = -\frac{1}{r}e^{-P_{s,1}r}(P_{s,2} + P_{s,3}r + P_{s,4}r^2), \quad (5)$$

$$h_{s's'}(r) = -e^{-(P_{s',1}r + P_{s',2}r^2 + P_{s',3}r^3)}(P_{s',4} + P_{s',5}r + P_{s',6}r^3 + P_{s',7}r^5 + P_{s',8}r^7 + P_{s',9}r^9), \quad (6)$$

$$\phi(r) = \frac{1}{r}e^{-P_{\phi,1}r}(P_{\phi,2} + P_{\phi,3}r + P_{\phi,4}r^2 + P_{\phi,5}r^3 + P_{\phi,6}r^4). \quad (7)$$

Although the binding energies of diatomic molecular and solid phases [body-centered-cubic (bcc) and face-centered-cubic (fcc) crystal structures] compared reasonably with first principles calculations<sup>19,20</sup> without the interaction between the  $s$  orbital and  $s'$  orbital, we found that the excited energy levels were unphysically close to the ground energy levels at very high density. To introduce the interaction between two orbitals we simply assume that  $h_{ss'}(r)$  is a linear combination of  $h_{ss}(r)$  and  $h_{s's'}(r)$ . We determined the coefficients by a qualitative fitting to the electronic density of states of hydrogen clusters obtained from the Hartree-Fock calculations.<sup>21</sup> Specifically, there is a repulsion between  $s$  and  $s'$  energy levels with the introduction of the nonzero  $h_{ss'}(r)$  term in the tight-binding Hamiltonian matrix. In the Hartree-Fock calculations, we obtained the electronic density of states of a hydrogen cluster ( $N=54$ ) with  $1s$  basis and  $1s-2s(p)$  basis separately. In this way we get the amount of the energy level shift between bonding and antibonding states. We performed the cluster calculations with and

without the  $h_{ss'}(r)$  term in the tight-binding method and adjusted the shift by varying the coefficients, fitting qualitatively to the Hartree-Fock result. The resulting form is

$$h_{ss'}(r) = 0.2h_{ss}(r) + 0.2h_{s's'}(r). \quad (8)$$

Finally, it was necessary to scale down  $h_{s's'}(r)$  by half and increase  $E_{ss'}$  to 1.5 Ry to obtain reasonable relative binding energies between diatomic molecular and solid phases of hydrogen. In Table I, we list all the resulting parameters for the new tight-binding model for hydrogen.

In Fig. 1, we show the radial dependences of the hopping matrix elements and the pair potential. We note that, by the nature of the fitting procedure, the  $s'$  orbital represents both the atomic  $2s$  and  $2p$  orbitals in a complicated way, although the notation implies a single  $2s$  orbital. To facilitate the molecular-dynamics simulations, the overlap integrals and the pair potential go smoothly to zero at  $r = 8$  bohrs. Specifically, for  $h_{\alpha\beta}(r)$  and  $\phi(r)$  we use

TABLE I. Parameters for the tight-binding model of hydrogen as defined in Eqs. (5)–(7).

$P_{s,1}$	1.1418475	$P_{s,2}$	0.0042828	$P_{s,3}$	0.737475
$P_{s,4}$	0.8154019				
$P_{s',1}$	-0.5784604	$P_{s',2}$	0.234274	$P_{s',3}$	-0.007893832
$P_{s',4}$	0.008104665	$P_{s',5}$	0.06333355	$P_{s',6}$	-0.014445175
$P_{s',7}$	0.00128827	$P_{s',8}$	$-0.3733631 \times 10^{-4}$	$P_{s',9}$	$0.47620535 \times 10^{-6}$
$P_{\phi,1}$	1.716997	$P_{\phi,2}$	1.984032	$P_{\phi,3}$	1.4063775
$P_{\phi,4}$	-1.23886	$P_{\phi,5}$	2.504998	$P_{\phi,6}$	-0.4479742

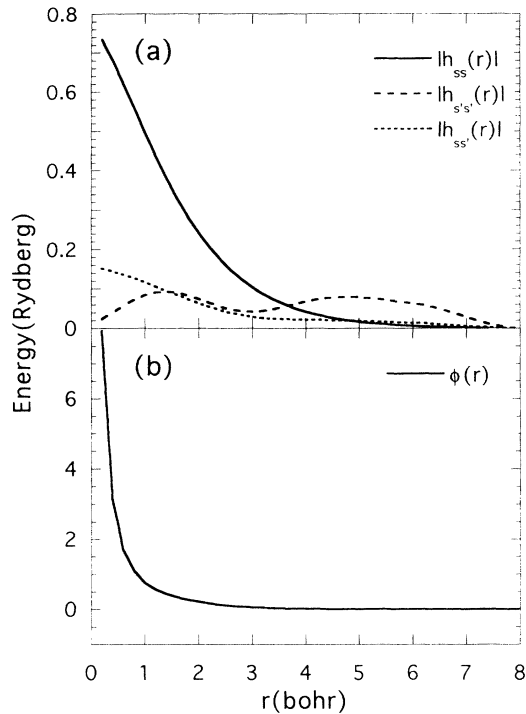


FIG. 1. (a) Radial dependence of the tight-binding hopping matrix elements as a function of separation  $r$  between atoms. (b) Radial dependence of the repulsive pair potential as a function of separation.

$$f(r) = a_0 + a_1(r - r_1) + a_2(r - r_1)^2 + a_3(r - r_1)^3$$

for  $r_1 < r < r_{\max}$ , (9)

which is required to go smoothly to zero at the designated cutoff distance  $r_{\max}$ . The four coefficients are determined by requiring that  $f(r)$  be continuous at  $r_1$  and zero at  $r_{\max}$ . In our tight-binding model for hydrogen, we chose  $r_1 = 6$  bohrs and  $r_{\max} = 8$  bohrs. In this way, all neighbor shells up to a distance of 8 bohrs are automatically included during simulations with no ambiguity in cutoff distances for different structures and phases.

In Fig. 2, we compare the binding energies of diatomic molecular and solid phases of hydrogen with the first principles calculations.<sup>19,20</sup> The binding energy of the diatomic hydrogen molecule at the equilibrium bond length 1.4 bohr is 2.305 eV/atom which is very close to the result of Kolos and Wolniewicz (2.373 eV/atom).<sup>19</sup> Although the equilibrium binding energies of bcc and fcc crystal structures relative to the diatomic molecule are very close to the values of the first principles calculations (1.394 eV/atom versus 1.320 for bcc and 1.391 versus 1.336 for fcc), equilibrium interatomic separations of this tight-binding model are longer than the first principles results (3.64 bohrs versus 2.95 for bcc and 3.82 bohrs versus 3.05 for fcc).<sup>20</sup> We also calculated the binding energy of the diamond structure as a function of interatomic distance and found the equilibrium energy 1.032 eV/atom higher than the diatomic phase at an interatomic separation of 2.94 bohrs, which is very close to the first

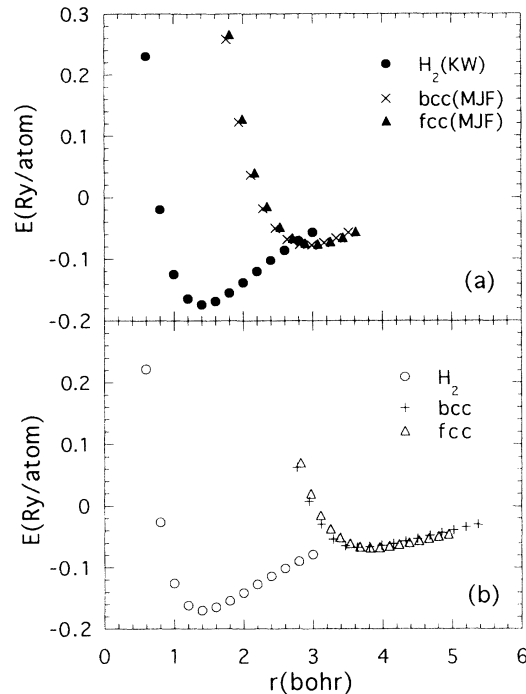


FIG. 2. Binding energy as a function of nearest-neighbor distance for diatomic molecule ( $H_2$ ), body-centered-cubic (bcc), and face-centered-cubic (fcc) crystal structures of hydrogen. (a) The results of Refs. 18 (KW) and 19 (MJF); (b) the results of the tight-binding model.

principles result obtained by Barbee and Cohen (1.139 eV/atom at 2.48 bohrs).<sup>22</sup>

### III. MOLECULAR-DYNAMICS SIMULATIONS OF HOT DENSE HYDROGEN

In order to test the tight-binding model, we have performed constant-volume, constant-temperature molecular-dynamics simulations with  $N$  hydrogen atoms in a cubic box with periodic boundary conditions. We started in a bcc or fcc structure with velocities determined randomly from a Boltzmann distribution at the desired temperature  $T$  and then equilibrated at  $T$  with a conventional velocity-scaling method. We also performed simulations with diamond structure to assure that the initial geometry played no role in the simulations. To introduce the effects of excited and continuum states, we invoke local thermodynamical equilibrium that sets the electron and ion temperatures equal. We populate the electronic states according to a Fermi-Dirac distribution at the ionic temperature. In the cases reported in this paper,  $N$  ranges from 128 to 686 depending on densities and temperatures in the simulations.<sup>23</sup> Time steps ranged from 0.073 to 0.29 fs, and total trajectory simulations varied between 150 and 700 fs.<sup>24</sup>

The calculated pair distribution function  $g(r)$  at low temperature (0.1 eV, 1160 K) is shown in Fig. 3.  $g(r)$  gives the probability of finding an atom at a distance  $r$  from a reference origin atom. At low densities, we ob-

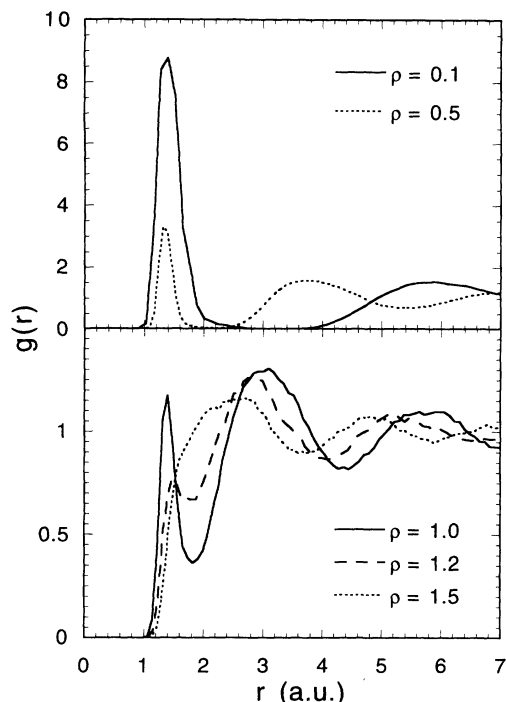


FIG. 3. Pair correlation function  $g(r)$  as a function of radial distance at  $T = 0.1$  eV and at densities  $\rho = 0.1, 0.5, 1.0, 1.2, 1.5$   $\text{g cm}^{-3}$  with the TBMD simulations.

serve a molecular fluid characterized by the distinctive peak of  $H_2$  at 1.4 bohr. As the density increases, the position of the first peak remains nearly the same, but the second peak moves significantly toward shorter distances. This indicates the change in intermolecular spacing due to the compression, as also observed in other studies.<sup>6,9</sup> At about  $\rho = 1.2$   $\text{g cm}^{-3}$  ( $r_s [\equiv (3/4\pi n)^{1/3}] = 1.31$ , corresponding to pressure  $\sim 300$  Gpa (Ref. 25)) we encounter the gradual disappearance of the molecular peak, inferring pressure dissociation. This transition comes at a slightly higher density than for the density-functional molecular-dynamics simulation with the local density approximation (LDA-MD).<sup>8,15</sup> To study the phase transition accurately at this temperature, we would need to include the zero-point motion of hydrogen, the energy of which is a few tenths of eV. However, we note that our results, obtained without the contribution of zero-point motion of hydrogen, compare very well with other results<sup>6,9</sup> using the same approximation.

Figure 4 shows the electronic density of states at  $\rho = 0.5, 1.0,$  and  $1.5$   $\text{g cm}^{-3}$ , indicating that atomic liquid hydrogen at high density is metallic, while at low density hydrogen is a molecular insulator. At low density (0.5  $\text{g cm}^{-3}$ ), there is a gap at the Fermi level, while there is no gap at high density (1.5  $\text{g cm}^{-3}$ ). At intermediate density (1.0  $\text{g cm}^{-3}$ ), we observe the closure of the gap, and hydrogen looks like a very poor metal with a very small number of states at the Fermi level.

We studied size effects in the MD simulations with our tight-binding model and found no dependence on the sample size. For example, we obtained the same result for both  $N = 250$  and  $N = 432$  (bcc-structure) supercell

calculations at  $\rho = 1.0$   $\text{g cm}^{-3}$ . In addition,  $N = 216$  diamond-structure and  $N = 256$  fcc-structure supercell calculations produced the same result. This insensitivity is crucial in representing very dense systems since finite size effects become larger as the density increases. For a comparison, we note that the Skinner-Pettifor model<sup>17</sup> showed size dependences in the MD simulations.<sup>8</sup> Also, there is no ambiguity of cutoffs in our model, while the TBMD results of the Skinner-Pettifor model show cutoff dependences.

In Fig. 5, we display the effects of temperature at a fixed density ( $\rho = 1$   $\text{g cm}^{-3}$ ). We observed a phase transition from molecular fluid to atomic fluid as we raised the temperature from 1160 to 60 000 K. Referring to the electronic density of states, hydrogen transforms to liquid metal at sufficiently high temperatures.

The coefficient of self-diffusion,  $D$ , provides an important measure of the dynamics in a hot dense plasma. In Fig. 6, we compare the self-diffusion coefficients of the TBMD simulations, obtained from the slope of the atomic mean-square displacement,<sup>26</sup> with the LDA-MD

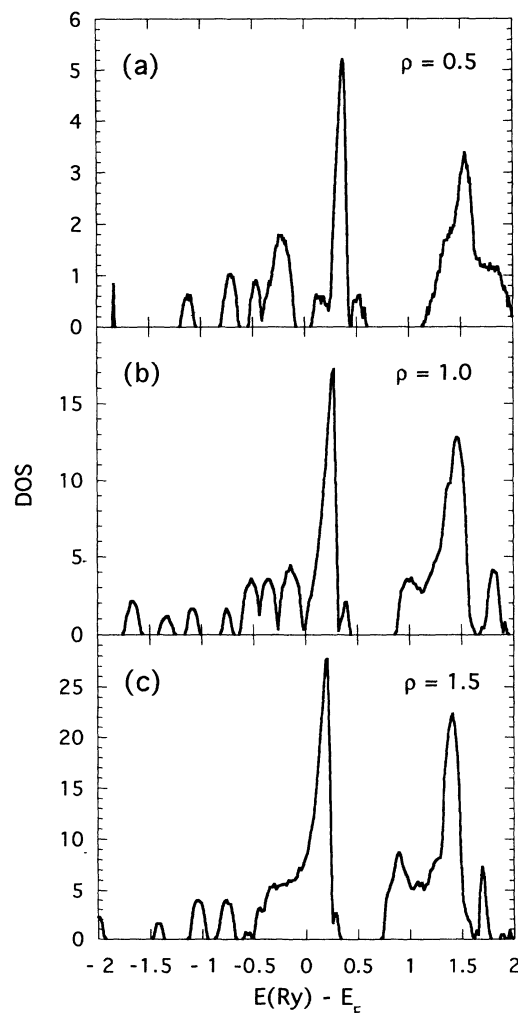


FIG. 4. Time-averaged electronic density of states in arbitrary units at  $T = 0.1$  eV and at  $\rho = 0.5$  (a), 1.0 (b), 1.5 (c)  $\text{g cm}^{-3}$ .

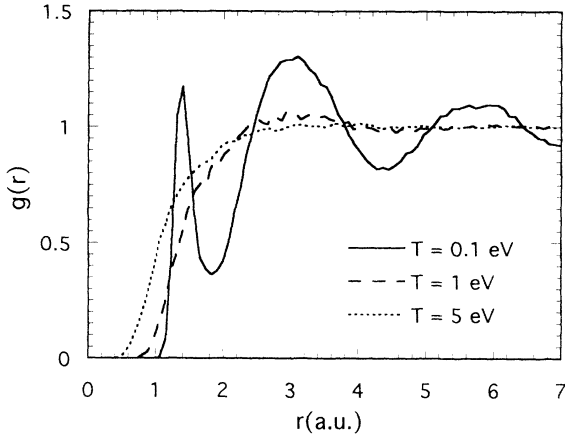


FIG. 5. Pair correlation function  $g(r)$  at density  $\rho = 1 \text{ g cm}^{-3}$  and at temperature  $T = 0.1, 1, 5 \text{ eV}$  with TBMD simulations.

results<sup>15</sup> and the OCP model.<sup>27</sup> The agreement between the TBMD and LDA-MD results is very good within statistical errors. However, at low temperature ( $T = 1 \text{ eV}$ ), the OCP values are significantly lower than the TBMD values for the whole range of density. At this temperature, the plasma coupling constant  $\Gamma (\equiv e^2/r_s k_B T)$ , which is the ratio of the Coulomb to thermal energy, ranges from 9 to 28. In such a strongly coupled plasma regime, the interatomic potential energy prevails over the thermal motion. However, our study indicates that quantum many-body effects still dominate over the bare Coulombic interactions. In the OCP theory, electrons are assumed to form a rigid, uniform background neutralizing the average space-charge field of the ions.

We note that all the cases in Fig. 6 correspond to an atomic fluid phase of hydrogen with no peak in  $g(r)$ . At very low density ( $\rho < 0.5 \text{ g cm}^{-3}$ ) and at low temperature ( $T = 1 \text{ eV}$ ), we observed the molecular fluid phase being stable. In this phase, the self-diffusion mechanism is different from the atomic diffusion.

As we increase the temperature, we observe better agreement between the OCP and TBMD results, as displayed in Figs. 6(b) and 6(c). Now  $\Gamma$  drops into the range of 2–6 at  $T = 5 \text{ eV}$  and the thermal effects clearly compete with the interatomic interactions. At this high temperature, the electrons form a smoother distribution that more resembles the OCP assumptions. Similar behavior was found by Younger<sup>28</sup> for He in which the self-diffusion coefficient obtained from the Hartree-Fock molecular-dynamics simulations became comparable to the OCP value at density about  $8 \text{ g cm}^{-3}$  at  $T = 5 \text{ eV}$ .

Zérah *et al.*<sup>10</sup> have performed molecular-dynamics simulations of the hydrogen plasma with the Thomas-Fermi theory (TFMD). To compare our TBMD model with the TFMD model, we have calculated the self-diffusion coefficients at  $\rho = 2.5 \text{ g cm}^{-3}$ . At  $T = 0.5 \text{ eV}$  ( $\Gamma \simeq 50$  and  $r_s \simeq 1$ ), we obtained  $D = 2.0 \times 10^{-3} \text{ cm}^2 \text{ s}^{-1}$ , which is twice the TFMD and thrice the OCP value. However, at higher temperature ( $T=2.5 \text{ eV}$ ,  $\Gamma \simeq 10$ ,  $r_s \simeq 1$ ), the TBMD value ( $D = 8.7 \times 10^{-3} \text{ cm}^2 \text{ s}^{-1}$ ) is only 11% larger than the TFMD and 47% larger than the OCP value. The Thomas-Fermi theory includes the inhomogeneity of the

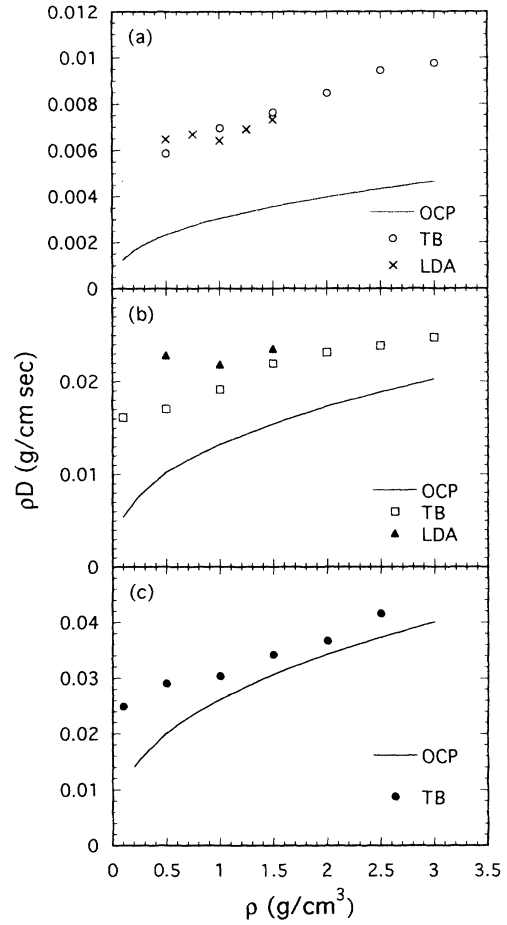


FIG. 6. Self-diffusion coefficient multiplied by density as a function of density. (a) At  $T = 1 \text{ eV}$ , with the LDA-MD (cross), the TBMD (open circle), and the OCP (solid line); (b) at  $T = 3 \text{ eV}$ , with the LDA-MD (triangle), the TBMD (square), and the OCP (solid line); (c) at  $T = 5 \text{ eV}$ , with the TBMD (solid circle) and the OCP (solid line).

electron gas simply by assuming uniform electron distributions locally in the inhomogeneous charge cloud, while the OCP theory assumes a homogeneity of the electron gas. Here, again, we observe the consistent phenomenon that the thermal excitation appears to provide a charge distribution characteristic of the simpler models.

#### IV. SUMMARY

In this paper, we have presented a tight-binding model for hydrogen. With the tight-binding molecular-dynamics simulations, we have studied the structure and dynamics of hot dense hydrogen plasmas at various densities and temperatures. Pair correlation functions and self-diffusion coefficients have been calculated and compared very well with the sophisticated density-functional molecular-dynamics results. At high temperature and high density, the self-diffusion coefficients of the TBMD simulations are comparable to the OCP values, while the difference is large at low temperature where quantum many-body effects are dominant. Work on mixtures of hydrogen isotopes is forthcoming.

## ACKNOWLEDGMENTS

This work was performed under the auspices of the U.S. Department of Energy through Los Alamos Na-

tional Laboratory (LANL). We thank R. L. Martin (Los Alamos) for his help with the CI calculations, and acknowledge a grant of time on the LANL IBM workstation cluster.

- 
- <sup>1</sup> J. Nuckolls, L. Wood, A. Thiessen, and G. Zimmerman, *Nature* **239**, 139 (1972); J. D. Lindl, R. L. McCoy, and E. M. Campbell, *Phys. Today* **45**(9), 32 (1992); W. J. Hogan, R. Bangester, and G. L. Kulcinski, *Phys. Today* **45**(9), 42 (1992).
- <sup>2</sup> H. Iyetomi and S. Ichimaru, *Phys. Rev. A* **34**, 3203 (1986).
- <sup>3</sup> D. J. Stevenson, *Annu. Rev. Earth Planet. Sci.* **10**, 2571 (1982).
- <sup>4</sup> S. Ichimaru, *Rev. Mod. Phys.* **54**, 1017 (1982).
- <sup>5</sup> G. Chabrier, N. W. Ashcroft, and H. E. DeWitt, *Nature* **360**, 48 (1992).
- <sup>6</sup> S. M. Younger, in *Radiative Properties of Hot Dense Matter*, edited by W. Goldstein, C. Hooper, J. Gauthier, J. Seely, and R. Lee (World Scientific, Singapore, 1991), p. 137.
- <sup>7</sup> J. Theilhaber, *Phys. Fluids B* **4**, 2044 (1992).
- <sup>8</sup> L. A. Collins, J. D. Kress, D. L. Lynch, and N. Troullier, *J. Quant. Spectrosc. Radiat. Transfer* **51**, 65 (1994).
- <sup>9</sup> D. Hohl, V. Natoli, D. M. Ceperley, and R. M. Martin, *Phys. Rev. Lett.* **71**, 541 (1993).
- <sup>10</sup> G. Zérah, J. Clérouin, and E. L. Pollock, *Phys. Rev. Lett.* **69**, 446 (1992).
- <sup>11</sup> L. A. Collins and A. L. Merts, in *Radiative Properties of Hot Dense Matter*, edited by J. Davis, C. Hooper, R. Lee, A. Merts, and B. Rozsnyai (World Scientific, Singapore, 1985), p. 385.
- <sup>12</sup> K. Fujima, T. Watanabe, and H. Adachi, *Phys. Rev. A* **32**, 3583 (1985).
- <sup>13</sup> D. A. Liberman, *Phys. Rev. B* **20**, 4981 (1979).
- <sup>14</sup> C. Z. Wang, C. T. Chan, and K. M. Ho, *Phys. Rev. B* **39**, 8586 (1989); I. Kwon, R. Biswas, C. Z. Wang, K. M. Ho, and C. M. Soukoulis, *Phys. Rev. B* **49**, 7242 (1994), and references therein.
- <sup>15</sup> I. Kwon, L. A. Collins, J. D. Kress, N. Troullier, and D. L. Lynch, *Phys. Rev. E* **49**, R4771 (1994).
- <sup>16</sup> L. Collins, J. Kress, I. Kwon, D. Lynch, and N. Troullier, in *American Physical Society Proceedings of Topical Conference on Atomic Processes in Plasmas* (in press).
- <sup>17</sup> A. J. Skinner and D. G. Pettifor, *J. Phys. Condens. Matter* **3**, 3029 (1991).
- <sup>18</sup> B. H. Lengsfeld III, R. L. Martin, P. W. Saxe, T. V. Russo, M. Page, B. Schneider, M. O. Braunstein, P. J. Hay, and A. K. Rappe, computer code MESA, 1993.
- <sup>19</sup> W. Kolos and L. Wolniewicz, *J. Chem. Phys.* **43**, 2429 (1965).
- <sup>20</sup> B. I. Min, H. J. F. Jansen, and A. J. Freeman, *Phys. Rev. B* **30**, 5076 (1984).
- <sup>21</sup> M. J. Frisch, G. W. Trucks, M. Head-Gordon, P. M. W. Gill, M. W. Wong, J. B. Foresman, B. G. Johnson, H. B. Schlegel, M. A. Robb, E. S. Replogle, R. Gomperts, J. L. Andres, K. Raghavachari, J. S. Binkley, C. Gonzalez, R. L. Martin, D. J. Fox, D. J. Defrees, J. Baker, J. J. P. Stewart, and J. A. Pople, computer code GAUSSIAN 92, revision B, Gaussian Inc., Pittsburgh PA, 1992.
- <sup>22</sup> T. W. Barbee III and M. Cohen, *Phys. Rev. B* **44**, 11 563 (1991).
- <sup>23</sup> For example, at low density and high temperature, a large  $N$  was used since the self-diffusion coefficient was expected to be high.
- <sup>24</sup> To avoid possible problems caused by large steps in small cells, small time steps were used on small  $N$  systems.
- <sup>25</sup> The density-pressure conversion was obtained by using the relation in R. J. Hemley, H. K. Mao, L. W. Finger, A. P. Jephcoat, R. M. Hazen, and C. S. Zha, *Phys. Rev. B* **42**, 6458 (1990).
- <sup>26</sup> M. P. Allen and D. J. Tildesley, *Computer Simulation of Liquids* (Oxford Science, Oxford, 1987).
- <sup>27</sup> J. P. Hansen, I. R. McDonald, and E. L. Pollock, *Phys. Rev. A* **11**, 1025 (1975).
- <sup>28</sup> S. M. Younger, *Phys. Rev. A* **45**, 8657 (1992).